

Research Article

## Fluid-Attenuated Inversion Recovery Sequence in MRI in Distinguishing Fluid Cyst from Tumor in the Brain

Kawthar Shafiq Ahmed Mohammed<sup>1</sup>, Nabil Saleh Abdullah Nasser<sup>2</sup>

<sup>1</sup>Department of Physics, Faculty of Sciences, University of Aden, Yemen

<sup>2</sup>Department of Physics, Faculty of Education, University of Aden, Yemen.

<https://doi.org/10.47372/uajnas.2024.n1.a09>

### ARTICLE INFO

Received: 17 July 2024

Accepted: 14 Aug. 2024

#### Keywords:

*Nuclear Magnetic Resonance, Fluid Attenuated Inversion Recovery, Fast Spin Echo, fluid cyst.*

### Abstract

Nuclear magnetic resonance (NMR) is a physical phenomenon used to investigate the characteristics of atomic nuclei. It is the absorption and emission of energy by nuclei in a magnetic field, which can offer extensive information on the structure, dynamics, reaction state, and chemical environment of molecules. Magnetic Resonance Imaging (MRI) is the safest imaging method. It gives a visual representation of human tissue without surgical intervention for clinical diagnosis. In this research, Fast Spin Echo (SE), Multi-Slice Spin Echo (MSSE), and Fluid Attenuated Inversion Recovery (FLAIR) sequences were used. The case under study is placed in an i-open permanent MRI system type in order to image a brain lesion. The obtained signals are encoded to fill k-space through the three stages, i.e., slice selection, phase encoding and frequency. The MRI-processed brain image is reconstructed by inverse Fourier transform in order to find the location of the cyst, and T1 weighted, T2 weighted, and FLAIR tests were performed to obtain three types of images. The images were compared with normal images in each type of applied sequence. Subsequently, the fluid signal was specifically attenuated in the targeted location to help distinguish between a tumor and fluid in the transverse relaxation time-weighted image. The signal was attenuated in the designated location, turned black, and appeared the color of free water, like cerebrospinal fluid, indicating that it was a fluid rather than a tumor. Consequently, a cyst fluid lesion is detected. Our study establishes a foundation for utilizing free fluid signal attenuation to differentiate between cyst fluid and tumors when other sequences fail to do the same..

### 1. Introduction

In the 1930s, the term Nuclear Magnetic Resonance (NMR) was coined by physicist Isidor Rabi, who won the Nobel Prize in 1944 [1, 2]. NMR is a spectroscopic technique that exploits the magnetic properties of atomic nuclei. It involves the study of the interaction between nuclear spins and an applied magnetic field. Protons within a nucleus possess unique spin and charge distributions, which endow them with magnetic characteristics. When subjected to a strong external magnetic field, these nuclei absorb specific frequencies of electromagnetic energy, a phenomenon known as resonance. This energy absorption is characteristic of the nucleus and its molecular environment, providing valuable insights into molecular structure and composition [3, 4]. The foundational principles of NMR were established in 1946 by Swiss-American physicist

Felix Bloch and American physicist Edward Purcell, who independently investigated the magnetic properties of nuclei in solids and liquids. Their groundbreaking work earned them the Nobel Prize in Physics in 1952 [5, 6]. A pivotal moment in medical imaging occurred in 1960, when Raymond Damadian discovered distinct NMR characteristics between normal and cancerous tissues. Utilizing the newly developed NMR spectrometer, he observed that differences in relaxation times between these tissues were significant [7]. This revolutionary finding put the foundation for the development of Magnetic Resonance Imaging (MRI) as a diagnostic tool. The technique was developed in 1973 by American chemist Lauterbur and British physicist Mansfield; they were awarded the 2003 Nobel Prize in Medicine and Physiology [8]. In a significant improvement, Paul Lauterbur proposed a method to create two-dimensional anatomical images by

\* Correspondence to: Department of Physics, Faculty of Science, University of Aden- Yemen  
E-mail address: [Kawthar.shafeeq.scie@aden-univ.net](mailto:Kawthar.shafeeq.scie@aden-univ.net)

mapping the interior of the body using gradients in the magnetic field acting as a secondary magnetic field [9]. Regarding Mansfield, he investigated nuclear magnetic resonance diffraction in solid materials and then scanned and obtained higher-resolution images using mathematical techniques [10]. When magnetic resonance systems were first commercialized in the early 1980s [11], the term "nuclear magnetic resonance" was dropped due to public associations with nuclear weapons. To emphasize the imaging capabilities of the technology and distance it from these negative connotations, the name was changed to "Magnetic Resonance Imaging" (MRI) [1]. MRI is a modern, reliable, and safe imaging technique. Unlike CT scans and X-rays, which employ ionizing radiation, MRI utilizes radio waves and magnetic fields to produce detailed images of the body's internal structures. MRI has replaced numerous invasive and ionizing radiation-based diagnostic methods, significantly reducing patient risk. MRI is based on the interaction of hydrogen's magnetic properties with a large external magnetic field and radio waves, resulting in extremely detailed images of the internal human body [12–14].

The human body contains approximately 70% water. The water molecule is made up of an oxygen atom and two hydrogen atoms, and this makes it an abundant source of hydrogen nuclei [15]. The hydrogen nucleus ( $H^1$ ) has magnetic properties; each hydrogen nucleus acts as a tiny magnet [16], and this is what makes it affected when placed in a strong magnetic field and exposed to radio waves [17]. Hydrogen nuclei possess magnetic moments due to their intrinsic spin property. Nevertheless, its net magnetization in the human body equals zero because their spin orientations are randomly arranged. If the human body is placed in a strong external field, the hydrogen nuclei's magnetic moments align with the external field parallel (a little bit more) and anti-parallel to the external field. This creates a net magnetization parallel to the external field, which is called a longitudinal magnetization, which is responsible for acquiring the images of the tissues of the human body [18, 19]. MRI systems comprise several key components: powerful magnets, gradient coils, radiofrequency (RF) coils, a sophisticated computer system, and a patient table [20].

The T1 and T2 relaxation times and the concentration of hydrogen protons in the fluid flow determine the signal intensity and brightness of pixels. The tissues under examination can be shown as high-resolution sectional pictures with significant contrast between damaged and healthy tissue [21]. MRI's diagnostic precision depends on the imaging sequence parameters that are chosen to improve image quality. Many sequences, such as spin echo, multiple slice spine echo, and FLAIR, can be

employed to raise the caliber of clinical information that can be deduced from an MR image [22]. MRI images reflect anatomical location, morphological features, and characterize pathological tissues [23–25]. Recently the fluid attenuation inversion recovery (FLAIR) sequence, which was designed to null signals from the cerebrospinal fluid (CSF), For fat and cerebrospinal fluid (CSF), there are differences in the signal intensity relative to the inversion time (TI) [26–33]. As a result, lesions' intensities varied qualitatively according to the type of the sequence [34]. This study aims to detect brain fluid cysts using MRI with a FLAIR sequence. Moreover, the research seeks to establish the most effective MRI sequence for diagnosing a particular brain disorder.

Bhargav et al. [31] studied the utility of contrast-enhanced fluid-attenuated inversion recovery (FLAIR) in MRI and Compared results with contrast-enhanced T1-weighted image in different intracranial lesions. They used Forty-nine patients with known intracranial lesions that underwent a gadolinium agent. Their results were that FLAIR images are useful in intra-axial lesions and not useful in extra-axial lesions. Sahu et al. [22] searched on the comparison between spin echo T2-weighted and fluid-attenuated inversion recovery for characterizing brain pathology. They used 0.2 Tesla open-resistive MRI on twenty cases of different brain pathologies. They found the FLAIR sequence is more beneficial than the T2 sequence. Le et al. [34] searched about the mismatch between T2 and fluid-attenuated inversion recovery in tumefactive multiple sclerosis. They tested one case of a 46-year-old male with tumefactive multiple sclerosis. They found the T2-FLAIR mismatch sign wasn't a differential feature between glioma and tumefactive demyelination. Aprile et al. [35] studied intracranial lesions performed with conventional techniques and FLAIR. They used forty-five cases of different cystic intracranial lesions and applied T1-weighted, T2-weighted, FLAIR, and PD-weighted sequences. They concluded that the FLAIR sequence was better for imaging intracranial lesions. Mohammed and Nasser [36] accurately detected and diagnosed the glioblastoma multiform in the FLAIR image for on a 70-year-old man. And the edge was identified in Gd-T1-weighted image and FLAIR. The examination was performed with the aid of 0.5 T i-open permanent MRI system.

## 2. Materials and methods:

The present study was carried out at the department of radiology, Aden German International Hospital in the city of Aden. The MRI unit was an open-type 0.5 Tesla manufactured by China Resources Wandong Medical Equipment Co. LTD (Figure 1). A description of

components and composition of the MRI system is detailed elsewhere [37]. The case of brain pathology in a 4-year-old male child who weighs 40 Kg was studied using an open permanent magnet with a magnet field strength of  $(0.5 \pm 5\%)$  Tesla. The signal intensity and characteristics have been compared in T1WI, T2WI, and FLAIR. During the experiment, the patient studied using multi-slice spin echo, spin echo, and FLAIR sequences in different planes (sagittal, transversal and coronal). Then, the images were studied.

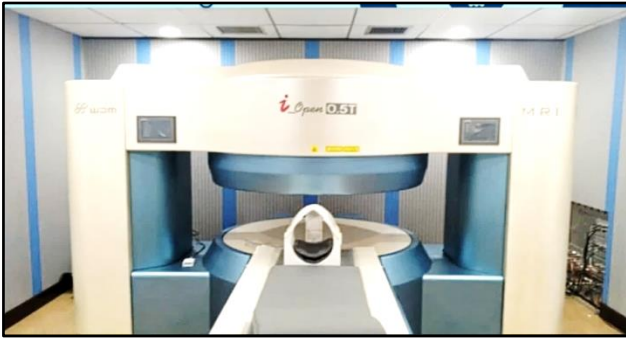


Figure 1: i-open permanent MRI system

Prior to MRI scanning, patients were carefully screened to exclude any ferromagnetic objects or implanted medical devices, such as pacemakers or cochlear implants that could pose risks within the magnetic field. All MRI safety protocols were strictly observed. The patient must remain completely still so that there is no interference that would affect the quality of the imaging. Since the studied case is a child, he was anesthetized. The patient is inserted into the middle of the magnetic field to ensure the uniformity and homogeneity of the primary magnetic field, using the laser identification located within the device.

First, the human body is placed in the primary magnetic field. Next, we apply the RF pluses of a specific sequence to flip longitudinal magnetization to the transverse plane XY by using RF coils, and relaxation occurs when RF pluses stop. Then, the RF coils measure the signal resulting from transverse magnetization; this allows to measure an analog complex echo signal that induces an electrical current in the radio frequency coils installed in the head. After that, the mathematical Fourier transform is used to separate the analog complex signal recorded by the radio frequency coils into its primary frequencies and then encode them to fill k-space through the slice selecting, phase & frequency encoding stages. Finally, after filling the K space and processing the image, we apply the inverse Fourier transform to reconstruct the MRI brain images in order to find the location of the body.

In the three tests, three types of images were obtained using the general parameters: slice thickness of 6 mm, spacing between slices of 7.2 mm, flip angel of  $90^\circ$ , and pixel bandwidth of 108.5069 HZ.

### 2.1 First test

In this test, we will try to obtain a T1-weighted image to evaluate the image using a multi-slice spin echo (MSSE) sequence. The sequence included in the protocol was as follows: repetition time (TR) 630 ms, echo time (TE) 16 ms, echo number 131, number of phase encoding steps 131, and echo train length 1.

### 2.2 Second test

This second test is to obtain a T2-weighted image to be able to evaluate the image. The sequence included in the protocol was as follows: repetition time (TR) 5610 ms, echo time (TE) 138 ms, echo number 14, number of phase encoding steps 149, and echo train length 11.

### 2.3 Third test

The third test FLAIR sequence is used when the previous two tests fail to evaluate the images. As the fluid is attenuated by calculating the inversion time – the time during which the fluid signal is zeroed – we can know the inversion time by knowing the longitudinal relaxation time (T1) of the tissue whose signal is to be zeroed. The sequence included in the protocol was as follows: repetition time (TR) 9382 ms, echo time (TE) 115ms, inversion time (TI) 2334 ms, echo number 18, number of phase encoding steps 152, and echo train length 9.

## 3. Results and Discussions

Three distinct MRI sequences were employed to generate images that precisely delineate the lesion's location and its impact on surrounding tissues, as illustrated in the figures below:

### 3.1 Multi Slice Spin Echo Sequence (MSSE)

In this sequence we obtain a T1- weighted image (T1WI) by using a short TR = 630 ms and a short TE = 16 ms spin echo sequence. Fluids in this sequence appear dark and the fats appear bright, as shown in Figure 2.

### 3.2 Spin Echo sequence (SE):

This sequence produced a T2-weighted image (T2WI) using a spin echo sequence with a long TR and long TE. In this sequence, fluids and lesions appear bright because they

have long TR = 5610 ms and long TE = 138 ms, while fats and proteins appear dark because they have short TR and short TE, as shown in Figure 3.

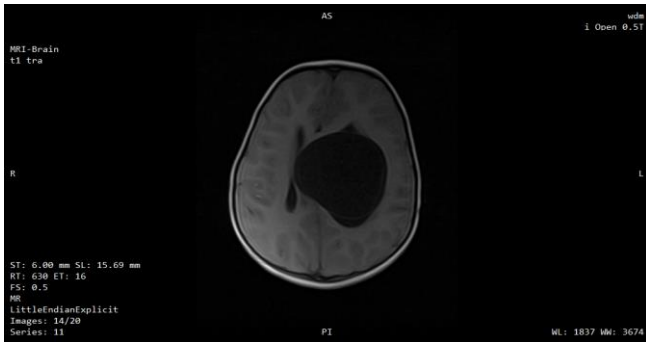


Figure 2: T1-weighted image of the brain on transverse plane (Test1)

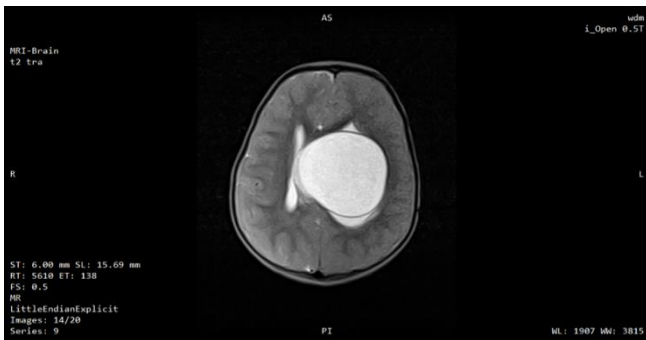


Figure 3: T2-weighted image of the brain on transverse plane (Test2)

### 3.3 Fluid Attenuation Inversion Recovery (FLAIR)

To distinguish the lesion from cyst fluid, a FLAIR sequence was implemented. This fast spin-echo technique employed a 180° pulse with extended TR of 9382 ms, TE of 115 ms, and TI of 2334 ms to effectively suppress the cyst fluid signal. The resulting image exhibited T2-like characteristics but free fluids are dark, as depicted in Figure 4.

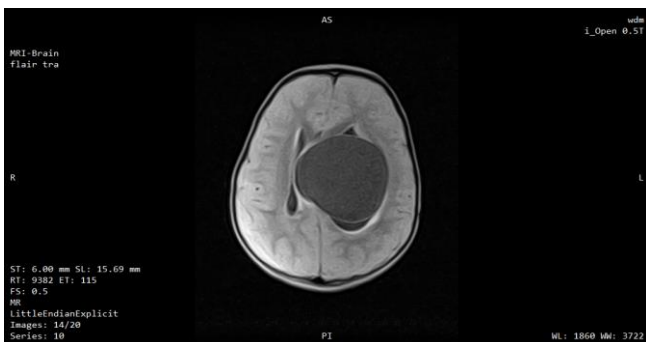


Figure 4: FLAIR-image of the brain on transverse plane (Test3).

Subsequent to acquiring the aforementioned MRI sequences, a comparative analysis was conducted between the obtained images and corresponding normal reference images for each sequence. In the normal image, fluids have a long T1 (to recover their longitudinal magnetization). But the T1-weighted image uses a short TR, so the fluids in the image appear dark. As in cerebrospinal fluid (CSF). Signal of fats and proteins: In the normal image, fats and proteins have a short T1 to restore their longitudinal magnetization, so although the TR is short in the T1WI-weighted image, therefore the signal is still high and the fats and proteins appear bright, as shown in Figure 5.

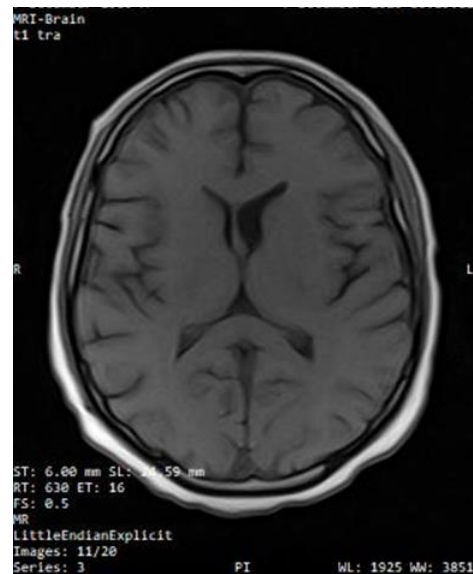


Figure 5: T1-weighted image of normal brain on transverse plane

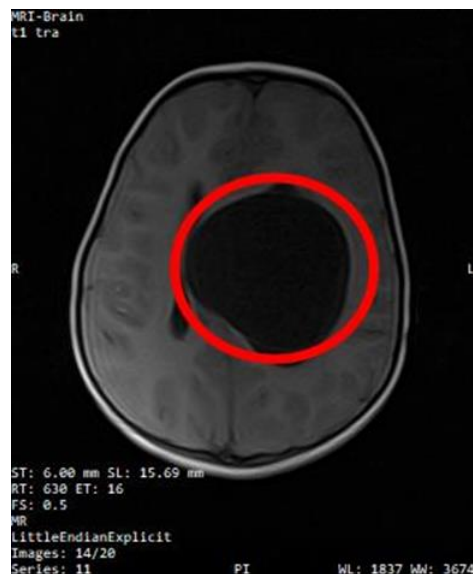


Figure 6: T1-weighted image of abnormal brain, where the image highlights the abnormal tissues (red circle)

In the abnormal image, the fat signal and the water signal appear as in the normal condition, except for the area marked with a red circle (Figure 6). The water signal and the fat signal appear as in the normal case, except for the area marked with a red circle that appears dark in black and gives the same water signal (the CSF signal).

In the normal image, fluids have a long T2 (when their transverse magnetization is lost). They retain their magnetism for a long time, and the recorded signal is strong, so the fluids in the image appear bright. As in cerebrospinal fluid (CSF). Signal of fats and proteins: In the normal image, fats and proteins contain a short T2 when their transverse magnetization decays. Therefore, they lose their magnetization quickly, and the recorded signal is weak and appears dark in the image, as shown in Figure 7.

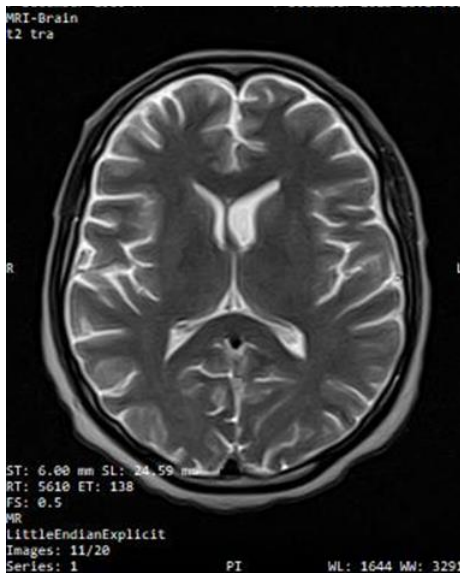


Figure 7: T2-weighted image of Normal brain on transverse plane

In the abnormal image, the fat signal and the water signal appear as in the normal case, except for the area marked with a red circle (Figure 8). The water signal and the fat signal appear as in the normal case, except for the area marked with a red circle that appears bright and gives the same water signal (the CSF signal).

In the normal image, when the FLAIR sequence is used to suppress the fluid signal, by using fast spin echo-inversion recovery (FSE-IR), the sequence will be under the condition of keeping T2 contrast and restrain the signal of free water. This is done by applying a 180-RF pulse to flip the longitudinal magnetization (MZ) to the negative pole (M-z), by recovering the magnetization during relaxation, it will reach zero before becoming positive again. At this point, when a 90-RF pulse is applied, it will not create magnetization in the transverse plane of the free

liquid. This in turn leads to the cancellation of the free fluid signal as in cerebrospinal fluid (CSF). FLAIR image is similar to the weighted image transverse relaxation (T2WI) time in the spin echo sequence, except that the free fluid appears black and the restricted fluid appears white, as shown in Figure 9.

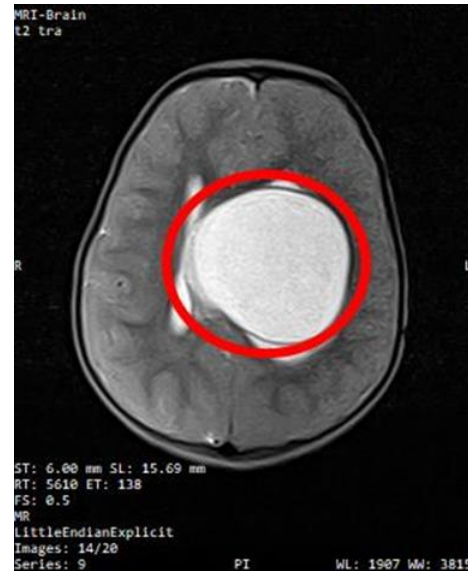


Figure 8: T2-weighted image of abnormal brain, where the image highlights the abnormal tissues (red circle).

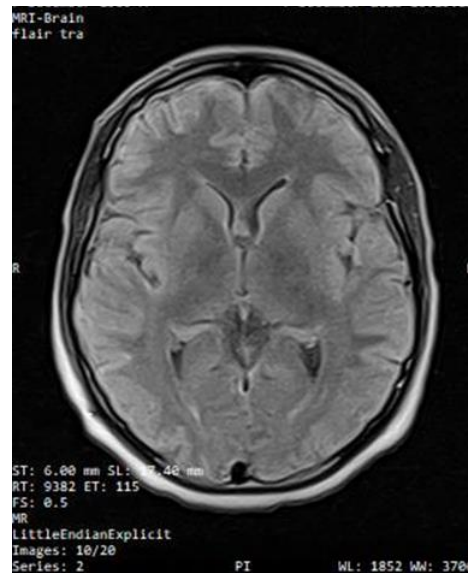
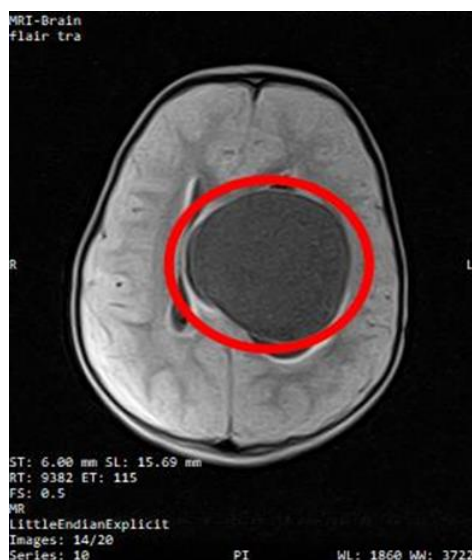


Figure 9: FLAIR-image of normal brain on transverse plane

A third test was used in order to differentiate whether the brightness in the transverse relaxation time-weighted image (T2WI) was a tumor or a fluid. Following signal attenuation of free fluid, the lesion also exhibited signal suppression, appearing dark on the image (Figure 10). This dark signal intensity resembled that of cerebrospinal fluid,

indicating a fluid-filled lesion rather than a tumor. The effective attenuation of the free fluid signal was crucial in distinguishing between a tumor and a cystic lesion. The study findings confirmed the effectiveness of the FLAIR sequence in detecting the intracranial lesions and are in agreement with literature [22, 35]. On the other hand, in our previous study, the lesion signal was not attenuated in the FLAIR image, which made the abnormal brain tissue appear bright, and the tumor was identified [36].



**Figure 10:** FLAIR-Image of abnormal brain, where the image highlights the abnormal tissues (red circle)

### Conclusion

This research utilized SE, MSSE, and FLAIR sequences to image a brain lesion in an i-open MRI system. This study demonstrated the effectiveness of FLAIR MRI in accurately diagnosing a brain fluid cyst in a 4-year-old male patient. Inverse Fourier transform was employed to reconstruct the MRI-processed brain image for cyst localization. T1-weighted, T2-weighted, and FLAIR images were acquired and compared to corresponding normal images for analysis. While T1-weighted and T2-weighted imaging provided preliminary information, they were insufficient for definitive characterization of the lesion. In contrast, FLAIR imaging effectively suppressed the signal from the cyst fluid, clearly differentiating it from surrounding tissues. These findings underscore the importance of FLAIR as a valuable tool for the diagnosis of fluid cysts in patient's brain. Future studies could investigate the potential of advanced MRI techniques, such as diffusion-weighted imaging (DWI) in conjunction with FLAIR could provide additional insights into the nature and characteristics of intracranial fluid lesions.

### References

1. K. A. Joyce, "From numbers to pictures: The development of magnetic resonance imaging and the visual turn in medicine," *Sci Cult (Lond)*, vol. 15, no. 1, pp. 1–22, Mar. 2006, doi: 10.1080/09505430600639322.
2. A. Filler, "The History, Development and Impact of Computed Imaging in Neurological Diagnosis and Neurosurgery: CT, MRI, and DTI," *Nature Precedings*, May 2009, doi: 10.1038/npre.2009.3267.1.
3. A. J. Olaide, E. Olugbenga, and D. Abimbola, "A Review of the Application of Nuclear Magnetic Resonance in Petroleum Industry," *International Journal of Geosciences*, vol. 11, no. 04, pp. 145–169, 2020, doi: 10.4236/ijg.2020.114009.
4. Ě. Kupče, L. Frydman, A. G. Webb, J. R. J. Yong, and T. D. W. Claridge, "Parallel nuclear magnetic resonance spectroscopy," *Nature Reviews Methods Primers*, vol. 1, no. 1, p. 27, Apr. 2021, doi: 10.1038/s43586-021-00024-3.
5. R. Kleinberg and J. Jackson, "An Introduction to the History of NMR Well Logging," *Concepts Magn Reson*, vol. 13, no. 6, pp. 340–342, 2001.
6. A. Macovski, "MRI: A charmed past and an exciting future," *Journal of Magnetic Resonance Imaging*, vol. 30, no. 5, pp. 919–923, Nov. 2009, doi: 10.1002/jmri.21962.
7. G.-H. Jahng, S. Park, C.-W. Ryu, and Z.-H. Cho, "Magnetic Resonance Imaging: Historical Overview, Technical Developments, and Clinical Applications," *Progress in Medical Physics*, vol. 31, no. 3, pp. 35–53, Sep. 2020, doi: 10.14316/pmp.2020.31.3.35.
8. J. Polzehl and K. Tabelow, "Magnetic Resonance Imaging in a Nutshell," 2019, pp. 5–14. doi: 10.1007/978-3-030-29184-6\_2.
9. J. Tourais, C. Coletti, and S. Weingärtner, "Brief Introduction to MRI Physics," in *Advances in Magnetic Resonance Technology and Applications*, 2022, pp. 3–36. doi: 10.1016/B978-0-12-822726-8.00010-5.
10. S. Mayor, "Nobel prize in medicine awarded to MRI pioneers," *BMJ*, vol. 327, no. 7419, pp. 827–827, Oct. 2003, doi: 10.1136/bmj.327.7419.827.
11. P. Rinck, "A short history of magnetic resonance imaging," *SPECTROSCOPYEUROPE*, vol. 20, no. 1, pp. 7–9, 2008.
12. M. Idress, "AN OVERVIEW ON MRI PHYSICS AND ITS CLINICAL APPLICATIONS," *National Journal of Current Pharmaceutical & Clinical Research*, vol. 4, no. 4, pp. 185–193, 2014.
13. S. Hussain et al., "Modern Diagnostic Imaging Technique Applications and Risk Factors in the Medical Field: A Review," *Biomed Res Int*, vol. 22, no. 1, pp. 1–19, Jun. 2022, doi: 10.1155/2022/5164970.
14. L. K. Niraj, "MRI in Dentistry- A Future Towards Radiation Free Imaging – Systematic Review," *JOURNAL OF CLINICAL AND DIAGNOSTIC RESEARCH*, vol. 10, no. 10, 2016, doi: 10.7860/JCDR/2016/19435.8658.
15. Y. Gossuin, H. Aline, P. Giilis, and L. Quoc, "Physics of magnetic resonance imaging: from spin to pixel," *J Phys D Appl Phys*, vol. 43, no. 21, 2010, [Online]. Available: <https://hal.science/hal-00569611>
16. D. B. Plewes and W. Kucharczyk, "Physics of MRI: A primer," *Journal of Magnetic Resonance Imaging*, vol. 35, no. 5, pp. 1038–1054, May 2012, doi: 10.1002/jmri.23642.
17. D. Wayne, "An Introduction to Magnetic Resonance Imaging Physics," University of Tennessee, Knoxville, 2000.
18. G. Katti, S. Ara, and A. Shireen, "Magnetic Resonance Imaging (MRI)-A Review," *INTERNATIONAL JOURNAL OF DENTAL CLINICS*, vol. 3, no. 1, pp. 65–70, 2011.
19. S. Currie, N. Hoggard, I. J. Craven, M. Hadjivassiliou, and I. D. Wilkinson, "Understanding MRI: basic MR physics for physicians," *Postgrad Med J*, vol. 89, no. 1050, pp. 209–223, Apr. 2013, doi: 10.1136/postgradmedj-2012-131342.
20. A. Shah and S. Aran, "A Review of Magnetic Resonance (MR) Safety: The Essentials to Patient Safety," *Cureus*, Oct. 2023, doi: 10.7759/cureus.47345.

21. N. Rehab, Y. Siwar, and Z. Mourad, "Machine Learning for Epilepsy: A Comprehensive Exploration of Novel EEG and MRI Techniques for Seizure Diagnosis," *J Med Biol Eng*, vol. 44, no. 3, pp. 317–336, Jun. 2024, doi: 10.1007/s40846-024-00874-8.
22. I. D. Sahu, S. Aryal, S. L. Shrestha, and R. K. Ghimire, "Comparison of Fluid Attenuated Inversion Recovery Sequence with Spin Echo T2-Weighted MRI for Characterization of Brain Pathology," *ArXiv*, Nov. 2009.
23. W. Mustafa, S. Ali, N. Elgendy, S. Salama, L. El Sorogy, and M. Mohsen, "Role of contrast-enhanced FLAIR MRI in diagnosis of intracranial lesions," *Egypt J Neurol Psychiatr Neurosurg*, vol. 57, no. 1, p. 108, Dec. 2021, doi: 10.1186/s41983-021-00360-x.
24. B. Jeong et al., "T1-weighted FLAIR MR Imaging for the Evaluation of Enhancing Brain Tumors: Comparison with Spin Echo Imaging," *Journal of the Korean Society of Magnetic Resonance in Medicine*, vol. 18, no. 2, pp. 151–156, 2014, doi: 10.13104/jksmrm.2014.18.2.151.
25. S. F. Elkholy, M. A. Sabet, M. E. Mohammad, and R. E. I. Asaad, "Comparative study between double inversion recovery (DIR) and fluid-attenuated inversion recovery (FLAIR) MRI sequences for detection of cerebral lesions in multiple sclerosis," *Egyptian Journal of Radiology and Nuclear Medicine*, vol. 51, no. 1, p. 188, Dec. 2020, doi: 10.1186/s43055-020-00298-9.
26. M. Symms, "A review of structural magnetic resonance neuroimaging," *J Neurol Neurosurg Psychiatry*, vol. 75, no. 9, pp. 1235–1244, Sep. 2004, doi: 10.1136/jnnp.2003.032714.
27. E. K. Lee, E. J. Lee, S. Kim, and Y. S. Lee, "Importance of Contrast-Enhanced Fluid-Attenuated Inversion Recovery Magnetic Resonance Imaging in Various Intracranial Pathologic Conditions," *Korean J Radiol*, vol. 17, no. 1, pp. 127–141, 2016, doi: 10.3348/kjr.2016.17.1.127.
28. K. Yalcinoz, T. Ikizceli, S. Kahveci, and O. I. Karahan, "Diffusion-weighted MRI and FLAIR sequence for differentiation of hydatid cysts and simple cysts in the liver," *Eur J Radiol Open*, vol. 8, 2021, doi: 10.1016/j.ejro.2021.100355.
29. Y. Baba and M. Niknejad, "Fluid attenuated inversion recovery," *Radiopaedia.org*.
30. M. Hasegawa, M. Sugiyama, N. Murata, M. Nagamoto, and T. Gomi, "FLAIR in Gd-EOB-DTPA Enhanced MRI: Does It Make a Difference?," *Open J Radiol*, vol. 07, no. 02, pp. 130–142, 2017, doi: 10.4236/ojrad.2017.72015.
31. R. Bhargava, A. Patil, V. Bakshi, T. Kalekar, and S. Gandage, "Utility of contrast-enhanced fluid-attenuated inversion recovery in magnetic resonance imaging of intracranial lesions," *West Afr J Radiol*, vol. 25, no. 1, pp. 34–38, 2018, doi: 10.4103/wajr.wajr\_4\_17.
32. S. C. Kim et al., "Contrast-Enhanced FLAIR (Fluid-Attenuated Inversion Recovery) for Evaluating Mild Traumatic Brain Injury," *PLoS One*, vol. 9, no. 7, 2014, doi: 10.1371/journal.pone.0102229.
33. M. L. White et al., "Fluid-attenuated inversion-recovery MR imaging in assessment of intracranial oligodendrogliomas," *Computerized Medical Imaging and Graphics*, vol. 29, no. 4, pp. 279–285, 2005, doi: 10.1016/j.compmedimag.2004.10.005.
34. D. Le, K. Trinh, N. Das, and A. H. Kuo, "T2-fluid attenuated inversion recovery mismatch in tumefactive multiple sclerosis," *BJR|case reports*, vol. 9, no. 1, Jan. 2023, doi: 10.1259/bjrcr.20220138.
35. I. Aprile et al., "Analysis of cystic intracranial lesions performed with fluid-attenuated inversion recovery MR imaging," *AJNR Am J Neuroradiol*, vol. 20, no. 7, pp. 1259–67, 1999.
36. K. Mohammed and N. Nasser, "Using MRI to detect and diagnose glioblastoma multiform," *Journal of the Faculties of Education - Aden* (in press).
37. Wandong Products Specification (WDM), "Technical Description i\_Open 0.5T Permanent MRI System." [Online]. Available: [https://expansionmedicalconsulting.com/wp-content/uploads/2020/03/WDM-Spec\\_i\\_Open-0.5T-201912.pdf](https://expansionmedicalconsulting.com/wp-content/uploads/2020/03/WDM-Spec_i_Open-0.5T-201912.pdf).



## مجلة جامعة عدن للعلوم الطبيعية والتطبيقية

Journal homepage: <https://uajnas.adenuniv.com>



بحث علمي

### تسلسل توهين السائل باستعادة الانقلاب في التصوير بالرنين المغناطيسي للتمييز بين كيس السائل والورم في الدماغ

كوثر شفيق أحمد محمد<sup>1</sup>، نبيل صالح عبدالله ناصر<sup>2</sup>

<sup>1</sup>قسم الفيزياء – كلية العلوم – جامعة عدن – اليمن  
<sup>2</sup>قسم الفيزياء – كلية التربية – جامعة عدن – اليمن

<https://doi.org/10.47372/uajnas.2024.n1.09>

مفاتيح البحث	الملخص
<p>التسليم: 17 يوليو 2024 القبول: 14 أغسطس 2024</p> <p><b>كلمات مفتاحية:</b> الرنين المغناطيسي النووي، توهين السائل باستعادة الانقلاب، صدى الغزل السريع، كيس السائل.</p>	<p>الرنين المغناطيسي النووي (NMR) هو ظاهرة فيزيائية تستخدم لفحص خصائص النوى الذرية، وهو عبارة عن امتصاص وانبعثات الطاقة بواسطة النوى في المجال المغناطيسي، والذي يمكن أن يوفر معلومات شاملة عن بنية الجزيئات وديناميكيتها وحالة التفاعل والبيئة الكيميائية للجزيئات. التصوير بالرنين المغناطيسي (MRI) هو أكثر طرق التصوير أماناً. يعطي تمثيلاً مرئياً للأنسجة البشرية دون تدخل جراحي للتشخيص السريري، في هذا البحث، تم استخدام تسلسلات صدى الدوران، وصدى الدوران متعدد الشرائح، وتوهين السائل باستعادة الانقلاب، حيث تم وضع الحالة قيد الدراسة بنظام التصوير بالرنين المغناطيسي الدائم ذات النوع المقنوح من أجل تصوير آفة الدماغ، يتم تفسير الإشارات التي تم الحصول عليها لملء مساحة <math>k</math> خلال المراحل الثلاث، أي اختيار الشريحة وترميز الطور والتردد، يتم إعادة بناء صورة الدماغ المعالجة بالرنين المغناطيسي عن طريق تحويل فورييه العكسي من أجل تحديد موقع الكيس، وتم إجراء اختبارات ترجيح زمن الاسترخاء الطولي وترجيح زمن الاسترخاء العرضي وتوهين السائل باستعادة الانقلاب للحصول على ثلاثة أنواع من الصور، تمت مقارنة الصور بالصور العادية في كل نوع من التسلسلات المطبقة، وبالتالي تم توهين إشارة السائل على وجه التحديد في الموقع المستهدف للمساعدة في التمييز بين الورم والسائل في الصورة الموزونة لزمن الاسترخاء العرضي. تم توهين الإشارة في المكان المحدد، وتحولت إلى اللون الأسود، وظهر لون الماء الحر، مثل السائل النخاعي، مما يدل على أنه سائل وليس ورماً، ونتيجة لذلك، تم الكشف عن آفة السائل الكيسي. تضع دراستنا أساساً لاستخدام توهين إشارة السائل الحرة للتمييز بين كيس السائل والأورام عندما تخفق التسلسلات الأخرى في تحديد الأمر ذاته.</p>